

# Effect of Sintering Temperature, $\text{Sm}^{3+}$ Concentration and Excitation Wavelength on Luminescence Properties in $\text{Eu}^{3+}$ Doped Strontium Tungstate Phosphors

Yan Dong REN<sup>1\*</sup>, Yong Hao LIU<sup>1</sup>, Shu Juan HAO<sup>1</sup>, Hai Ying CUI<sup>1</sup>, Hong Wei ZHANG<sup>1</sup>, Si Yu MENG<sup>2</sup>, Hong Yan DING<sup>3</sup>

<sup>1</sup> School of Physics and Electrical Information Engineering, Daqing Normal University, Daqing, China

<sup>2</sup> School of Chemistry, Chemical Engineering and Materials, Heilongjiang University, Harbin, China

<sup>3</sup> Daqing 28th high School, Daqing, China

**crossref** <http://dx.doi.org/10.5755/j01.ms.25.1.19032>

Received 13 September 2017; accepted 13 January 2018

The color-tunable  $\text{SrWO}_4:0.20\text{Eu}^{3+}$ ,  $\text{Sm}^{3+}$  phosphors are successfully prepared by co-precipitation method at a low temperature (800 °C). These phosphors can be efficiently excited by near-ultraviolet and blue light. The phase formation, luminescence properties, energy transfer between  $\text{Eu}^{3+}$  and  $\text{Sm}^{3+}$ , and the critical distance were studied. The  $\text{Sm}^{3+}$  ions as the sensitizer could extend the excitation spectrum and enhance emission. The CIE chromaticity coordinate was also presented. The emission hues covered the regions from pink, orange, to reddish-orange, and eventually to red, which can be controlled by adjusting excitation energy, calcination temperature, and doping rare earth ions ratio via the energy transfer. The high efficiency and high color purity red emitting  $\text{SrWO}_4:0.20\text{Eu}^{3+}$ ,  $x\text{Sm}^{3+}$  ( $x = 0.005 \div 0.01$ ) phosphors have higher color saturation than the commercially available  $\text{Y}_2\text{O}_3:\text{Eu}^{3+}$  red phosphor, which is in coincidence with the National Television Standard Committee system standard for red chromaticity (0.67, 0.33). The obtained phosphors exhibit an excellent light emitting efficiency, color-purity and lower correlated color temperature of the comfortable warm white LEDs.

**Keywords:** strontium tungstate, phosphors, color-tunable, warm white light emitting diodes.

## 1. INTRODUCTION

Strontium tungstate ( $\text{SrWO}_4$ ) has been widely used in optoelectronic industry and solid state laser system because of its interesting physicochemical properties, photocatalytic activity, cathodoluminescence, thermal expansion, and luminescence and so on. Recently,  $\text{Eu}^{3+}$  ions doped  $\text{SrWO}_4$  has been intensively researched as a red emitting phosphor for near ultraviolet (UV) and blue light-based white light emitting diodes (LEDs). They have been received widely attention recently due to their potential applications in catalysts, white LEDs, photoluminescent devices, solar cell, fluorescent lamps and more. Cavalcante et al. studied the Rietveld refinement and optical properties of  $\text{SrWO}_4:\text{Eu}^{3+}$  powders [1]. Hu et al. first observed the red afterglow of  $\text{Eu}^{3+}$  in  $\text{MWO}_4$  ( $\text{M} = \text{Sr}, \text{Ba}$ ) matrix [2]. There was an obvious charge imbalance in the lattice when  $\text{Eu}^{3+}$  ions were substituted for  $\text{Sr}^{2+}$  ions, which could affect the luminescence properties. The imbalance problem can be solved by charge compensation [3]. Among the trivalent rare-earth ( $\text{RE}^{3+}$ ) ions,  $\text{Sm}^{3+}$  ion is an excellent activator ion. For instance, one-dimensional  $\text{Sm}^{3+}$  doped  $\text{SrWO}_4$  with or without different charge compensation approaches (co-doping  $\text{Li}^+$ ,  $\text{Na}^+$  and  $\text{K}^+$ ) orange phosphor have been reported [4]. Sun et al. investigated the formation process and the electron trapping luminescence properties of  $\text{SrSO}_4:\text{Sm}^{3+}$  phosphors [5]. Liu et al. synthesized the reddish orange  $\text{Sm}^{3+}$ -doped  $\text{BaTiO}_3$  phosphors for white LEDs [6]. Singh et al. studied the predominant orange red light emission from  $\text{Sm}^{3+}$  doped  $\text{SrWO}_4$  phosphors [7].

Energy transfer (ET) from sensitizer to activator could enhance the emission of the activator. The energy can transfer from  $\text{Eu}^{3+}$  to  $\text{Sm}^{3+}$  in  $\text{SrWO}_4$  phosphors [8-10] and maybe it can enhance the photoluminescence (PL) properties of  $\text{SrWO}_4:\text{Eu}^{3+}$  phosphors.

In this work, the  $\text{SrWO}_4:\text{Eu}^{3+}$ ,  $\text{Sm}^{3+}$  phosphors were prepared by the simple coprecipitation method in air atmosphere. The phase structure, morphology, PL properties, Commission Internationale de l'Éclairage (CIE) 1931 x-y indexes and color temperature were investigated in detail. Moreover, the ET mechanism was discussed in detail, and the critical distance of ET was calculated. The CIE chromaticity coordinate was also presented.

## 2. EXPERIMENTAL

### 2.1. Preparation

A series of  $\text{Sm}^{3+}$ -doped  $\text{Sr}_{0.80}\text{WO}_4:\text{Eu}^{3+}_{0.20}$  phosphors were obtained by co-precipitation method from sodium tungstate dihydrate ( $\text{Na}_2\text{WO}_4 \cdot 2\text{H}_2\text{O}$ ) (99.99 % purity, Bailingwei Chemicals Co., Ltd., China), strontium nitrate [ $\text{Sr}(\text{NO}_3)_2$ ] (98 % purity, Beijing Yili Fina Chemicals Co., Ltd., China), europium oxide ( $\text{Eu}_2\text{O}_3$ ) (99.99 % purity, Haweiruike Chemicals Co., Ltd., China), samarium oxide ( $\text{Sm}_2\text{O}_3$ ) (99.99 % purity, Haweiruike Chemicals Co., Ltd., China), nitric acid ( $\text{HNO}_3$ ) (analytical grade, Bailingwei Chemical Reagent Co., Ltd., China) and polyethylene glycol ( $[\text{C}_4\text{H}_{10}\text{O}_3]_n$ ) as the starting materials. The molar concentration of the activator  $\text{Sm}^{3+}$  was varied from 0.1% to 5%. Firstly, according to  $\text{Sr}_{0.80}\text{WO}_4:\text{Eu}^{3+}_{0.20}$ ,  $\text{Sm}^{3+}_x$ , stoichiometric composition of  $\text{Na}_2\text{WO}_4 \cdot 2\text{H}_2\text{O}$  and  $\text{Sr}(\text{NO}_3)_2$  were dissolved in deionized water to form the

\* Corresponding author. Tel.: +0086-13845908460.  
E-mail address: [dqryd@163.com](mailto:dqryd@163.com) (Y.D. Ren)

aqueous solutions. Then stoichiometric  $\text{Eu}_2\text{O}_3$  and  $\text{Sm}_2\text{O}_3$  was dissolved in diluted  $\text{HNO}_3$  to offer the  $\text{Eu}^{3+}$  and  $\text{Sm}^{3+}$  ions, respectively. Afterwards mixing both of them together and adding dropwise into the  $\text{Sr}(\text{NO}_3)_2$  aqueous solution. The aqueous solution was stirred continuously for 30 min in ultrasound at the room temperature to assure a uniform dispersion. The mixture was dropped to a  $\text{Na}_2\text{WO}_4$  solution slowly. The PH of the solution was adjusted to a value within the range of 6 to 7 by addition of aqueous ammonia. The mixed solution was stirred for 60 min at room temperature to form a homogeneous solution.

The resulting precipitate was finally collected by many times centrifugation at 4500 rpm for 20 min and then dried at  $80^\circ\text{C}$  for 2 hours. After that, the mixture was grounded thoroughly in an agate mortar and introduced into a muffle furnace maintained at  $700\text{--}900^\circ\text{C}$  for 2 hours. Finally, the dried powders were ground lightly and used for characterization.

## 2.2. Characterizations

The crystal structure was identified by SHIMADZU X-ray diffraction (XRD)-6000 using  $\text{Cu K}\alpha$  radiation ( $\lambda = 1.5405 \text{ \AA}$ ). The field emission scanning electronic microscopy (FE-SEM) spectrum was measured using Hitachi S-4800. The excitation and emission spectra were recorded at room temperature using a Hitachi F-4500 with a Xe lamp.

## 3. RESULTS AND DISCUSSION

### 3.1. Structure and morphology

In order to characterize the crystal phase of the as-prepared powder samples, the XRD pattern of the  $\text{SrWO}_4:0.20\text{Eu}^{3+}, 0.01\text{Sm}^{3+}$  phosphors annealed at  $800^\circ\text{C}$  are presented in Fig. 1. All the strong diffraction peaks can be assigned to the pure tetragonal structure, following Joint Committee on Powder Diffraction Standards Card (JCPDS) No. 85-0587. Its lattice parameters are  $a = b = 5.416 \text{ \AA}$  and  $c = 11.95 \text{ \AA}$ . It can be considered that  $\text{Sm}^{3+}$  and  $\text{Eu}^{3+}$  have been effectively built into the  $\text{SrWO}_4$  host lattice because of no additional peaks of other phases have been observed in the as-obtained samples.

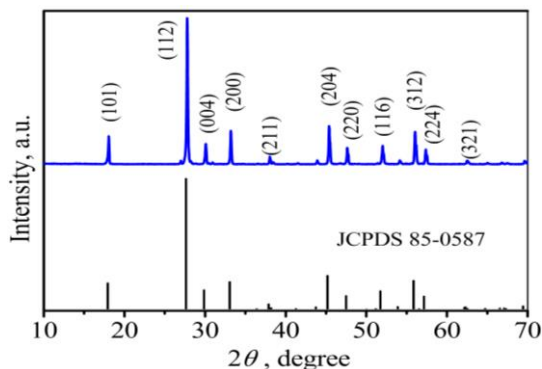


**Fig. 1.** The XRD pattern of  $\text{SrWO}_4:0.20\text{Eu}^{3+}, 0.01\text{Sm}^{3+}$  phosphors and the JCPDS No. 85-0587 database standard for  $\text{SrWO}_4$

The crystal structure of  $\text{SrWO}_4$  is shown in Fig. 2, The  $\text{SrWO}_4$  single crystal belongs to tetragonal sheelite structure with  $I4_1/a$  space group. The  $\text{WO}_4^{2-}$  tetrahedral

configuration is built up of hexavalent tungsten ( $\text{W}^{6+}$ ) surrounded by four oxygens (O) atoms in this crystal and divalent metal, strontium (Sr), shares corners with eight adjacent O sites, forming a  $[\text{WO}_4]^{2-}$  tetrahedron.

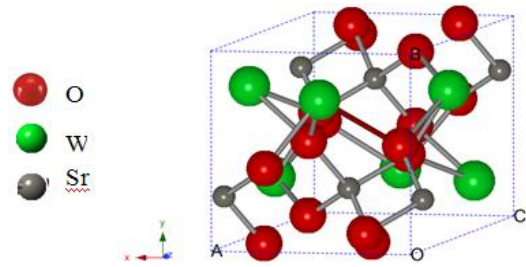


**Fig. 2.** View of the crystal structure of strontium tungstate

$\text{SrWO}_4$  almost remains its main crystal lattice structure when  $\text{Sr}^{2+}$  sites are substituted by other  $\text{RE}^{3+}$  ions. In this distorted dodecahedron geometry,  $\text{Sr}^{2+}$  and  $\text{RE}^{3+}$  atoms are coordinated to eight oxygen atoms considered as  $[\text{SrO}_8]$  and  $[\text{REO}_8]$  groups. Also, the slight shift of the XRD patterns of  $\text{SrWO}_4:0.20\text{Eu}^{3+}, 0.01\text{Sm}^{3+}$  relevant to the  $\text{SrWO}_4$  host can be observed and attributed to the different radii between  $\text{Sr}^{2+}$  ( $1.18 \text{ \AA}$ ) and rare earth ions [ $\text{Sm}^{3+}$  ( $0.96 \text{ \AA}$ ) and  $\text{Eu}^{3+}$  ( $0.95 \text{ \AA}$ ), which have the similar ionic radius].

The FE-SEM images for the  $\text{SrWO}_4:0.20\text{Eu}^{3+}, 0.01\text{Sm}^{3+}$  sample are shown Fig. 3. It can be clearly seen that the phosphors consist of large quantities of grains, and the average size of the grains is about  $3 \mu\text{m}$ . From the high magnification SEM, it can be seen the grains is anomalistic but the surface is smooth.

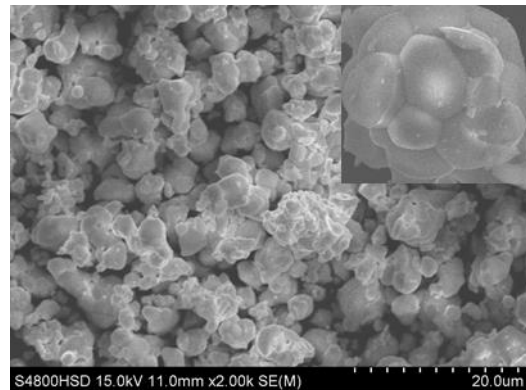


**Fig. 3.** SEM image of  $\text{SrWO}_4:0.20\text{Eu}^{3+}, 0.01\text{Sm}^{3+}$  particles

### 3.2. Photoluminescence properties

The excitation (left) and emission (right) spectra of  $\text{SrWO}_4:0.20\text{Eu}^{3+}, 0.01\text{Sm}^{3+}$  phosphors are presented in Fig. 4. Fig. 4 a shows the excitation (the black line under  $613 \text{ nm}$  excitation) and emission (the green, pink and red lines under  $465 \text{ nm}$ ,  $395 \text{ nm}$  and  $362 \text{ nm}$  excitation, respectively) spectra. The excitation spectrum is found to consist of a broad excitation band at about  $220\text{--}330 \text{ nm}$  and a series of much weaker electronic transitions of  $\text{Eu}^{3+}$  ( $4f^6$ ) in the longer wavelength region, which are listed in Table 1. Among these excitation transitions,  $395 \text{ nm}$  ( $^5\text{L}_6$ ),  $465 \text{ nm}$  ( $^5\text{D}_2$ ) and  $536 \text{ nm}$  ( $^5\text{D}_1$ ) lines are the most intense ones, which are assigned as the transitions from the  $^7\text{F}_0$  ground state to the different excited states of  $\text{Eu}^{3+}$ , respectively. In addition, the intensities of the f-f transition

emission for the  $\text{Eu}^{3+}$  ions are much higher than that of broadband, indicating that the excitation is mainly through the f-f transition emission of the  $\text{Eu}^{3+}$  ions.

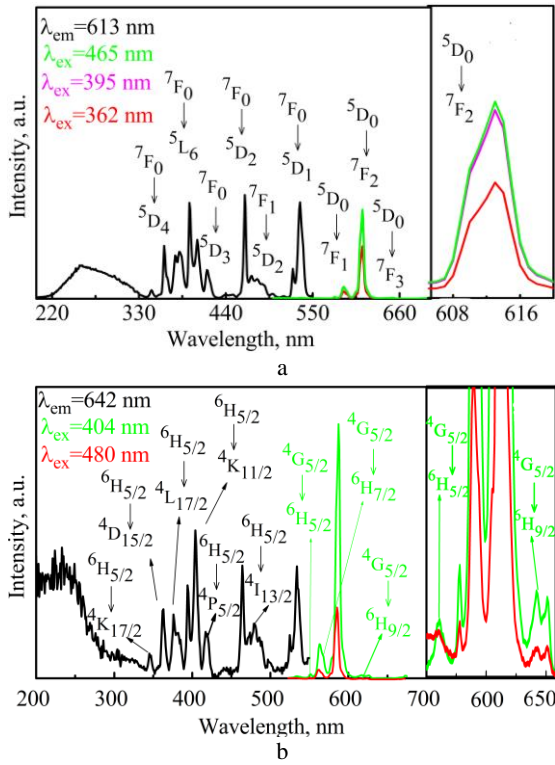


**Fig. 4.** The excitation and emission spectra of  $\text{SrWO}_4:0.20\text{Eu}^{3+}, 0.01\text{Sm}^{3+}$  phosphors under various excitation wavelengths. The insets show the enlarge views of diffraction peaks

**Table 1.** Transition energies of  $\text{Eu}^{3+}$  ions in excitation and emission spectra of  $\text{SrWO}_4:0.20\text{Eu}^{3+}, 0.01\text{Sm}^{3+}$  phosphors

Transitions	Excitation maximum, nm	Transitions	Excitation maximum, nm
${}^7\text{F}_0 \rightarrow {}^5\text{D}_4$	363 <sup>a</sup> , 367	${}^5\text{D}_0 \rightarrow {}^7\text{F}_1$	590
${}^7\text{F}_0 \rightarrow {}^5\text{L}_7$	377, 382 <sup>a</sup> , 385	${}^5\text{D}_0 \rightarrow {}^7\text{F}_2$	613
${}^7\text{F}_0 \rightarrow {}^5\text{L}_6$	395	${}^5\text{D}_0 \rightarrow {}^7\text{F}_3$	652
${}^7\text{F}_0 \rightarrow {}^5\text{D}_3$	416		
${}^7\text{F}_0 \rightarrow {}^5\text{D}_2$	465		
${}^7\text{F}_1 \rightarrow {}^5\text{D}_2$	474		
${}^7\text{F}_0 \rightarrow {}^5\text{D}_1$	527, 536 <sup>a</sup>		

<sup>a</sup> represents the predominant line in the group.

The emission spectra could be assigned to the characteristic transitions from the  ${}^5\text{D}_0$  to the  ${}^7\text{F}_J$  ( $J = 0, 1, 2, 3$  and  $4$ ). The highest emission peaks are located at 613 nm corresponding to the electric dipole  ${}^5\text{D}_0 \rightarrow {}^7\text{F}_2$  transition of  $\text{Eu}^{3+}$ . The higher ones are located at 590 nm corresponding to the parity allowed magnetic dipole transition of  ${}^5\text{D}_0 \rightarrow {}^7\text{F}_1$  line. Fig. 4 b shows the excitation (the black line under 642 nm excitation) and emission (the green and red lines under 404 nm and 480 nm excitation, respectively) spectra.

The excitation spectrum has a broad excitation band at about 200–310 nm, and it can be attributed to the charge transfer (CT) transition from  $\text{O}^{2-}-\text{Sm}^{3+}$  and  $\text{W}^{6+}-\text{O}^{2-}$ , and the intra-configurational f-f transitions of  $\text{Eu}^{3+}$  ions and the 4f–4f transitions of  $\text{Sm}^{3+}$  ions in the longer wavelength region, which are listed in Table 2.

**Table 2.** Transition energies of  $\text{Sm}^{3+}$  ions in excitation and emission spectra of  $\text{SrWO}_4:0.20\text{Eu}^{3+}, 0.01\text{Sm}^{3+}$  phosphors

Transitions	Excitation maximum, nm	Transitions	Excitation maximum, nm
${}^6\text{H}_{5/2} \rightarrow {}^4\text{K}_{17/2}$	346	${}^4\text{G}_{5/2} \rightarrow {}^6\text{H}_{5/2}$	560
${}^6\text{H}_{5/2} \rightarrow {}^4\text{D}_{15/2}$	362	${}^4\text{G}_{5/2} \rightarrow {}^6\text{H}_{7/2}$	595
${}^6\text{H}_{5/2} \rightarrow {}^4\text{L}_{17/2}$	376	${}^4\text{G}_{5/2} \rightarrow {}^6\text{H}_{9/2}$	641
${}^6\text{H}_{5/2} \rightarrow {}^4\text{K}_{11/2}$	404	${}^5\text{D}_0 \rightarrow {}^7\text{F}_1$	590
${}^6\text{H}_{5/2} \rightarrow {}^4\text{P}_{5/2}$	419	${}^5\text{D}_0 \rightarrow {}^7\text{F}_2$	613
${}^6\text{H}_{5/2} \rightarrow {}^4\text{I}_{13/2}$	480	${}^5\text{D}_0 \rightarrow {}^7\text{F}_3$	650

The  $\text{SrWO}_4:0.20\text{Eu}^{3+}, 0.01\text{Sm}^{3+}$  phosphor show not only the characteristic emission of  $\text{Eu}^{3+}$ , i.e.,  ${}^5\text{D}_0 \rightarrow {}^7\text{F}_1$  (the yellow light centered at 590 nm),  ${}^5\text{D}_0 \rightarrow {}^7\text{F}_2$  (the red band centered at 613 nm) and  ${}^5\text{D}_0 \rightarrow {}^7\text{F}_3$  (the red band centered at 650 nm), but also the characteristic emission of  $\text{Sm}^{3+}$ , i.e.,  ${}^4\text{G}_{5/2} \rightarrow {}^6\text{H}_{5/2}$ ,  ${}^4\text{G}_{5/2} \rightarrow {}^6\text{H}_{7/2}$  and  ${}^4\text{G}_{5/2} \rightarrow {}^6\text{H}_{9/2}$  transitions, as shown in the inset. The highest emission peak is located at 595 nm suggesting that  $\text{Sm}^{3+}$  ion replaces the  $\text{Sr}^{2+}$  ion in  $\text{SrWO}_4$  host. The emission intensity of  $\text{Sm}^{3+}$  ion is much stronger than that of  $\text{Eu}^{3+}$  ion.

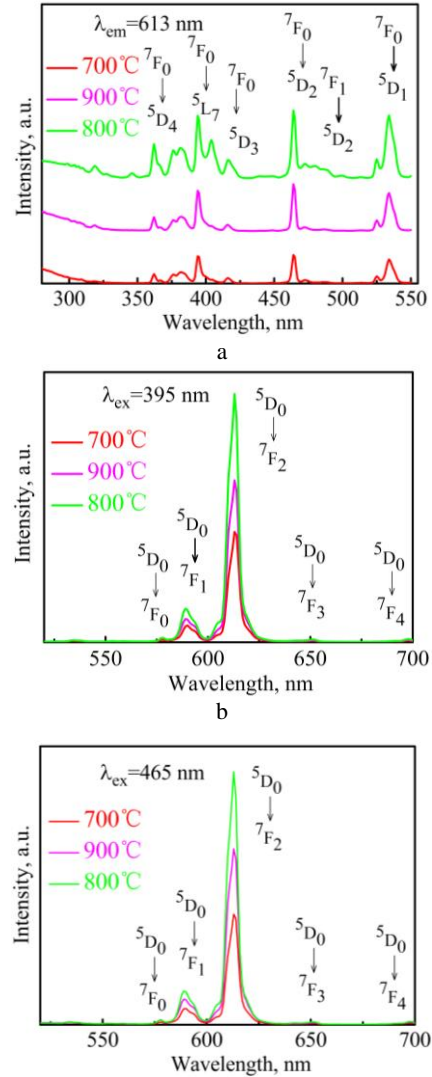


**Fig. 5.** PL spectra of the  $\text{SrWO}_4:0.20\text{Eu}^{3+}, 0.01\text{Sm}^{3+}$  phosphors annealed at different temperature for 2 h excited at 613 nm, 395 nm and 465 nm, respectively



**Table 3.** The CIE chromaticity coordinates and correlated color temperatures of SrWO<sub>4</sub>:0.20Eu<sup>3+</sup>, nSm<sup>3+</sup> (n = 0.001 ÷ 0.05) phosphors under various excitation wavelengths

Sample SrWO <sub>4</sub> :0.20Eu <sup>3+</sup> , nSm <sup>3+</sup>	CIE chromaticity coordinates (x, y) at different excitation wavelength			CCT (K) at different excitation wavelength		
	362 nm	395 nm	465 nm	362 nm	395 nm	465 nm
n = 0.001	(0.490, 0.343) yellowish-pink	(0.634, 0.363) reddish-orange	(0.614, 0.373) orange	1845	2171	1904
n = 0.003	(0.505, 0.301) pink	(0.635, 0.362) reddish-orange	(0.623, 0.370) reddish-orange	1899	2196	1989
n = 0.005	(0.545, 0.345) reddish-orange	(0.637, 0.361) reddish-orange	(0.671, 0.329) red	1776	2232	3728
n = 0.008	(0.567, 0.350) reddish-orange	(0.640, 0.358) reddish-orange	(0.672, 0.328) red	1835	2318	3797
n = 0.01	(0.618, 0.348) reddish-orange	(0.672, 0.327) red	(0.637, 0.360) reddish-orange	2272	3846	2250
n = 0.02	(0.534, 0.345) yellowish-pink	(0.638, 0.359) reddish-orange	(0.630, 0.366) reddish-orange	1754	2278	2092
n = 0.05	(0.526, 0.345) yellowish-pink	(0.632, 0.365) reddish-orange	(0.615, 0.378) orange	1749	2123	1870

$$y = \frac{Y}{X + Y + Z}, \quad (3)$$

where  $X$ ,  $Y$  and  $Z$  are the tristimulus values. Those values are given by the equations [17]:

$$X = \int_{\lambda} \bar{x}(\lambda) P(\lambda) d\lambda; \quad (4)$$

$$Y = \int_{\lambda} \bar{y}(\lambda) P(\lambda) d\lambda; \quad (5)$$

$$Z = \int_{\lambda} \bar{z}(\lambda) P(\lambda) d\lambda, \quad (6)$$

where  $\lambda$  is the wavelength of the equivalent monochromatic light.  $\bar{x}(\lambda)$ ,  $\bar{y}(\lambda)$  and  $\bar{z}(\lambda)$  are the color matching functions.  $P(\lambda)$  is the spectral power density.

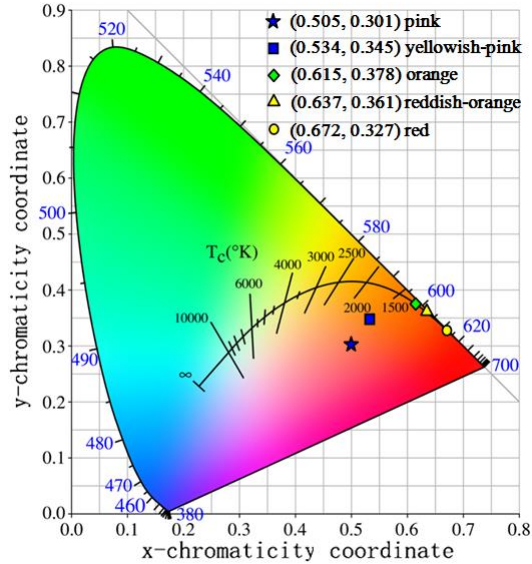


**Fig. 8.** CIE (x, y) chromaticity diagram for the emission spectra of SrWO<sub>4</sub>:0.20Eu<sup>3+</sup>, nSm<sup>3+</sup> (n = 0.003 ÷ 0.05) phosphor. The blue, yellow and green symbols denote the phosphor under 362 nm, 395 nm and 465 nm excitation, respectively

The blue, yellow and green symbols indicate the position of CIE chromaticity coordinates for SrWO<sub>4</sub>:0.20Eu<sup>3+</sup>, xSm<sup>3+</sup> (x = 0.001 ÷ 0.05) under 362 nm, 395 nm and 465 nm

excitation, respectively. A tunable color output in visible region by appropriately changing the ratio of doping rare earth ions concentration, excitation energy or calcination temperature. The emission hue can be varied from pink, yellowish-pink, orange, reddish-orange and eventually to red. These phosphors have higher color saturation than Y<sub>2</sub>O<sub>2</sub>S:Eu<sup>3+</sup> red phosphor. It is worth noting that the chromaticity coordinates (x, y) of SrWO<sub>4</sub>: 0.20Eu<sup>3+</sup>, xSm<sup>3+</sup> (x = 0.005 ÷ 0.01) phosphors are (0.67, 0.33) for the optimal Sm<sup>3+</sup> doping concentration, which coincide with the NTSC system standard red chromaticity (0.67, 0.33). When x = 0.01 molar, the color purity is calculated to be 99.2 %. These results strongly suggest that the novel red phosphor can be commercially utilized in blue LED-based white LEDs with higher Ra.

The CCT is used to characterize light sources by the simple formulas as follows [18]:

$$CCT = -437n^3 + 3601n^2 - 6861n + 5514.31; \quad (7)$$

$$n = \frac{x - x_e}{y - y_e}, \quad (8)$$

where the  $x_e = 0.3320$  and  $y_e = 0.1858$ . The color coordination and the CCT of phosphors are listed in Table 3. These results reveal that the CIE chromaticity coordinates of SrWO<sub>4</sub>:0.20Eu<sup>3+</sup>, xSm<sup>3+</sup> (x = 0.005 ÷ 0.01) is (0.67, 0.33) at white light CCT of about 3800 K. From these results, the Sm<sup>3+</sup> activated SrWO<sub>4</sub>:Eu<sup>3+</sup> can be commercially utilized in blue and near UV warm white LEDs with higher Ra.

#### 4. CONCLUSIONS

In summary, a series of novel color-tunable Sm<sup>3+</sup> activated SrWO<sub>4</sub>:0.20Eu<sup>3+</sup> phosphors are successfully prepared by the simple co-precipitation method at a low temperature (800 °C). The synthesis, structure, morphology, PL and CCT properties for the SrWO<sub>4</sub>:0.20Eu<sup>3+</sup>, xSm<sup>3+</sup> (x = 0.001 ÷ 0.05) phosphors was reported. The phosphors can be effectively excited by the light of near UV and blue LED. The optimum Sm<sup>3+</sup> doping concentration for SrWO<sub>4</sub>:0.20Eu<sup>3+</sup>, xSm<sup>3+</sup> phosphors were 0.01 molar. The investigation results demonstrated that the ET from Sm<sup>3+</sup> to

Eu<sup>3+</sup> arose from electric multipolar interaction with a critical distance of approximately 0.9277 nm. The CIE chromaticity coordinate was also presented. The red emitting SrWO<sub>4</sub>:0.20Eu<sup>3+</sup>, xSm<sup>3+</sup> (x = 0.005 ÷ 0.01) phosphors, which is in coincidence with the NTSC system chromaticity, have high efficiency, high color-purity, and higher color saturation than the commercially available Y<sub>2</sub>O<sub>2</sub>S:Eu<sup>3+</sup> red phosphor. In particular, we can appropriately tune color output by changing the ratio of doping rare earth ions concentration, excitation energy or calcination temperature. The obtained phosphors exhibit a high light emitting efficiency, good color-purity, and low CCT, which may be potentially applicable in comfortable warm white LEDs.

### Acknowledgments

This work is financially supported by a grant from the Instructional Technology Plan of Daqing City (Grant No.zd-2017-09) and Young Scholars of Daqing Normal University (Grant No. 14ZR22, 12ZR13, 14ZR16).

### REFERENCES

- Pereira, P.F.S., Nogueira, I.C., Longo, E., Nassar, E.J., Rosa, I.L.V., Cavalcante, L.S. Rietveld Refinement and Optical Properties of SrWO<sub>4</sub>:Eu<sup>3+</sup> Powders Prepared by the Non-Hydrolytic Sol-Gel Method *Journal of Rare Earths* 33 (2) 2015: pp. 113–128. [https://doi.org/10.1016/S1002-0721\(14\)60391-4](https://doi.org/10.1016/S1002-0721(14)60391-4)
- Kang, F.W., Hu, Y.H., Chen, L., Wang, X.J., Wu, H.Y., Mu, Z.F. Luminescent Properties of Eu<sup>3+</sup> in MWO<sub>4</sub> (M=Ca, Sr, Ba) Matrix *Journal of Luminescence* 135 (9) 2013: pp. 113–119. <https://doi.org/10.1016/j.jlumin.2012.10.041>
- Ren, Y.D., Liu, Y.H., Tan, S.M., Cui, H.Y., Wang, Y.L., Li, X.M., Yang, R., Wei, X., Zhang, H.W., Sun, Y.D. Energy Transfer Rate and Electron-Phonon Coupling Properties in Eu<sup>3+</sup>-doped Nanophosphors *Luminescence* 32 (3) 2017: pp. 425–433. <https://doi.org/10.1002/bio.3198>
- Xu, X.T., Zhao, S.Q., Liang, K.Y., Zeng, J.Y. Electrospinning Preparation and Luminescence Properties of One-dimensional SrWO<sub>4</sub>: Sm<sup>3+</sup> Nanofibers *Journal of Materials Science: Materials in Electronics* 25 (8) 2014: pp. 3324–3331. <https://doi.org/10.1007/s10854-014-2021-0>
- Sun, J.Y., Sun, G.C., Xue, B., Cui, D.P. Synthesis and Formation Process of SrSO<sub>4</sub>:Sm<sup>3+</sup> Phosphors with Hierarchical Structures and its Electron Trapping *Journal of Luminescence* 574 (48) 2013: pp. 560–564. <https://doi.org/10.1016/j.jallcom.2013.05.149>
- Zhang, L., Pan, H., Liu, H.G., Zhang, B.B., Jin, L., Zhu, M.H., Yang, W.Q. Theoretical Spectra Identification and Fluorescent Properties of Reddish Orange Sm-doped BaTiO<sub>3</sub> Phosphors *Journal of Alloys & Compounds* 643 (15) 2015: pp. 247–252. <https://doi.org/10.1016/j.jallcom.2015.04.087>
- Maheshwary Singh, B.P., Singh, R.A. Effect of Annealing on the Structural, Optical and Emissive Properties of SrWO<sub>4</sub>:Ln<sup>3+</sup> (Dy<sup>3+</sup>, Eu<sup>3+</sup> and Sm<sup>3+</sup>) Nanoparticles *Spectrochimica Acta Part A Molecular & Biomolecular Spectroscopy* 152 (5) 2016: pp. 199–207. <https://doi.org/10.1016/j.saa.2015.07.074>
- Xue, Y.N., Xiao, F., Zhang, Q.Y. Enhanced Red Light Emission from LaBSiO<sub>5</sub>:Eu<sup>3+</sup>, R<sup>3+</sup> (R= Bi or Sm) Phosphors *Spectrochimica Acta Part A Molecular & Biomolecular Spectroscopy* 78 (2) 2011: pp. 607–611. <https://doi.org/10.1016/j.saa.2010.11.030>
- Min, X., Huang, Z.H., Fang, M.H., Liu, Y.G., Tang, C., Wu, X.W. Energy Transfer from Sm<sup>3+</sup> to Eu<sup>3+</sup> in Red-Emitting Phosphor LaMgAl<sub>11</sub>O<sub>19</sub>:Sm<sup>3+</sup>, Eu<sup>3+</sup> for Solar Cells and Near-Ultraviolet White Light-Emitting Diodes *Inorganic Chemistry* 53 (12) 2014: pp. 6060–6065. <https://doi.org/10.1021/ic500412r>
- Jin, Y., Zhang, J.H., Hao, Z.D., Zhang, X., Wang, X.J. Synthesis and Luminescence Properties of Clew-like CaMoO<sub>4</sub>:Sm<sup>3+</sup>,Eu<sup>3+</sup> *Journal of Alloys & Compounds* 509 (38) 2011: pp. L348–L351. <https://doi.org/10.1016/j.jallcom.2011.07.047>
- Inokuti, M., Hirayama, F. Influence of Energy Transfer by the Exchange Mechanism on Donor Luminescence *Journal of Chemical Physics* 43 (6) 1965: pp. 1978–1989. <https://doi.org/10.1063/1.1697063>
- Xiong, J.H., Meng, Q.Y., Sun, W.J. Luminescent Properties and Energy Transfer Mechanism from Tb<sup>3+</sup> to Eu<sup>3+</sup> in CaMoO<sub>4</sub>:Tb<sup>3+</sup>, Eu<sup>3+</sup> Phosphors *Journal of Rare Earths* 34 (3) 2016: pp. 251–258. [https://doi.org/10.1016/S1002-0721\(16\)60022-4](https://doi.org/10.1016/S1002-0721(16)60022-4)
- Blasse, G. Energy Transfer Between Inequivalent Eu<sup>2+</sup> Ions *Journal of Solid State Chemistry* 62 (2) 1986: pp. 207–211. [https://doi.org/10.1016/0022-4596\(86\)90233-1](https://doi.org/10.1016/0022-4596(86)90233-1)
- Kumari, P., Manam, J. Enhanced Red Emission on Co-Doping of Divalent ions (M<sup>2+</sup>= Ca<sup>2+</sup>, Sr<sup>2+</sup>, Ba<sup>2+</sup>) in YVO<sub>4</sub>:Eu<sup>3+</sup> Phosphor and Spectroscopic Analysis for its Application in Display Devices *Spectrochimica Acta Part a Molecular & Biomolecular Spectroscopy* 152 (5) 2016: pp. 109–118. <https://doi.org/10.1016/j.saa.2015.07.039>
- Ren, Y.D., Liu, Y.H., Yang, R. A Series of Color Tunable Yellow-Orange-Red-Emitting SrWO<sub>4</sub>:RE (Sm<sup>3+</sup>, Eu<sup>3+</sup>-Sm<sup>3+</sup>) Phosphor for Near Ultraviolet and Blue Light-based Warm White Light Emitting Diodes *Superlattices and Microstructures* 91 2016: pp. 138–147. <https://doi.org/10.1016/j.spmi.2015.12.026>
- Mortimer, R.J., Varley, T.S. Quantification of Colour Stimuli Through the Calculation of CIE Chromaticity Coordinates and Luminance Data for Application Toinsitu Colorimetry Studies of Electrochromic Materials *Displays* 32 (1) 2011: pp. 35–44. <https://doi.org/10.1016/j.displa.2010.10.001>
- Dutta, S., Som, S., Sharma, S.K. Luminescence and Photometric Characterization of K<sup>+</sup> Compensated CaMoO<sub>4</sub>: Dy<sup>3+</sup> Nanophosphors *Dalton Transactions* 42 (26) 2013: pp. 9654–9661. <https://doi.org/10.1039/c3dt50780g>
- Kumar, J.S., Pavani, K., Babu, A.M., Giri, N.K., Rai, S.B., Moorthy, L.R. Fluorescence Characteristics of Dy<sup>3+</sup> Ions in Calcium Fluoroborate Glasses *Journal of Luminescence* 130 (10) 2010: pp. 1916–1923. <https://doi.org/10.1016/j.jlumin.2010.05.006>